Journal of the Korean Ceramic Society
Vol. 40, No. 4, pp. 393~397, 2003.

Role of AlN Piezoelectric Crystal Orientation in Solidly Mounted Film Bulk Acoustic Wave Resonators

Si-Hyung Lee, Sung Chul Kang, Sang Chul Han, Byung Kwon Ju,*
Ki Hyun Yoon, and Jeon-Kook Lee†**

Thin Film Materials Research Center, KIST, Seoul 136-791, Korea
**Microsystem Research Center, KIST, Seoul 136-791, Korea*
***Department of Ceramic Engineering, Yonsei University, Seoul 120-749, Korea*
(Received March 19, 2003; Accepted April 4, 2003)

ABATRACT

To investigate the effect of AlN c-axis orientation on the resonance performance of film bulk acoustic wave resonators, solidly mounted resonators with crystallographically different AlN piezoelectric films were prepared by changing only the bottom electrode surface conditions. As increasing the degree of c-axis texturing, the effective electromechanical coupling coefficient $(k_{eff})^2$ in resonators increased gradually. The least 4 degree of full width at half maximum in an AlN (002) rocking curve, which corresponds to k_{eff}^2 of above 5%, was measured to be necessary for band pass filter applications in wireless communication system. The longitudinal acoustic wave velocity of AlN films varied with the degree of c-axis texturing. The velocity of highly c-axis textured AlN film was extracted to be about 10200 m/s by mathematical analysis using Matlab.

Key words : AlN, Solidly mounted resonator, Effective coupling coefficient, Rocking curve, Acoustic wave velocity

1. Introduction

The interest in the thin Film Bulk Acoustic Wave Resonators(FBARs) acoustically isolated from substrates has recently been stimulated by modern trends in the development of communication systems such as the handling of higher frequency and its higher reliability, the improvement in electrical parameters and miniaturization. FBARs are well fit to this requirements.[1-6] Among the candidate piezoelectric materials for FBARs, AlN and ZnO thin films have been used successfully as the piezoelectric layer in FBARs.[5] Ferroelectric $PbZr_{1-x}Ti_xO_3$(PZT) series was also adopted for piezoelectric layer in FBARs due to the higher electromechanical coupling coefficients.[6] In this report, we used the reactively sputtered AlN piezoelectric film due to some demerits of ZnO and PZT films, such as lower longitudinal acoustic wave velocity, semiconducting properties of ZnO and piezoelectric properties dependence of PZT on the substrate properties.[7]

The basic structure of a FBAR is a piezoelectric film sandwiched between two electrodes. But, the practical FBARs require acoustic isolation from the substrate to prevent any energy leakage. There are two types of FBAR in methodology to make the extremes of mechanical impedance that tend to keep the wave confined within a desired volume.[1] One is the so-called Solidly Mounted Resonator(SMR). The acoustic isolation from the substrate can be obtained by means of a Bragg reflector that is composed of several pairs of quarter wavelength layers with the high acoustic impedance contrast. The second structure takes advantage of the low acoustic impedance of air or vacuum and needs either bulk or surface micromachining in order to create an air gap between substrates and resonating films. The SMR structure is favorable for integration and can be fabricated on a wide variety of substrates. Multiple reflections from the interfaces form a standing wave approximating a free surface reflection. If the layers are composed of altering low and high mechanical impedance materials, the reflections are large and the effect is to reduce the substrate impedance to near zero.

In bulk acoustic wave resonators, the piezoelectric coupling constant (k_t) of piezoelectric films determines the maximum bandwidth of FBAR Band Pass Filters(BPF).[8] In hexagonal AlN piezoelectric films, the higher degree of c-axis texturing, the higher k_t due to the highest value of piezoelectric constant along c-axis. However, influences of the degree of c-axis texturing of AlN films on the resonance properties of SMRs have not been reported in detail so far. Therefore, the knowledge of the correlation between the c-axis texturing of AlN films and achievable bandwidth is great importance.

In this study, the relationship between the achievable bandwidth of BPFs and the degree of AlN c-axis orientation in SMRs will be investigated. The degree of c-axis texturing of AlN films was controlled only by changing the bottom

†Corresponding author : Jeon-Kook Lee
E-mail : jkleemc@kist.re.kr
Tel : +82-2-958-5563 Fax : +82-2-958-6851

electrode surface conditions. And, the acoustic wave velocity of AlN piezoelectric films will also be extracted by mathematical analysis.

2. Experimental Procedures

Resonators composed of AlN thin film with top and bottom metal films were deposited on the Bragg reflector. To make the Bragg reflector, W and SiO_2 of quarter wavelength thickness were in-situ deposited on the Si (100) substrate by dc and rf magnetron sputtering, respectively. The impedances of W and SiO_2 were approximately 101.5 and 12.7 (units of 10^6 kg/m^2s), respectively.[1] AlN and Mo were chosen as a piezoelectric layer and an electrode, respectively. The aluminum nitride thin films were deposited by an rf magnetron sputtering system with a base pressure of 5×10^{-8} Torr. The rf discharge power was 550 W with less than 1% reflected power by using a reactive Ar/N_2 gas mixture with 20% N_2. The sputtering pressure was chosen to be 10 mTorr. A 3 inch diameter Al target with a purity of 99.999% was used with a cathode to substrate distance of 8 cm. The substrate was not heated and only depended on self-heating of the plasma. In order to control the degree c-axis texturing of AlN films, Mo bottom electrodes were deposited on the Bragg reflector by changing the sputtering pressures as mentioned in our earlier report.[9]

After making reflector layers, a bottom Mo electrode was deposited and etched. AlN and top Mo electrode were deposited and patterned by wet etching. The active area of resonators was chosen to be $200\times200\ \mu m^2$ for the 50 Ω impedance matching with measuring system for 1.9 GHz range. The impedance of FBAR was dependent on the area, as described in our other report in detail.[10] The degree of c-axis orientation of the AlN film was analyzed by X-Ray Diffraction (XRD) and rocking curve. The thicknesses and microstructures of the films were observed using a field emission Scanning Electron Microscope (SEM; Hitachi). For the measurement of the electromagnetic wave reflection S_{11}, the HP8753ES network analyzer was used. Before the measurements, the microwave probes and the network analyzer were properly calibrated. The calibration was performed for each sample and frequency band measurement. Using the obtained S-parameters, all other parameters of the structure such as the magnitude of electric impedance and the phase of electric impedance were calculated. Matlab and HP-ADS programs are then used to create a relational data-

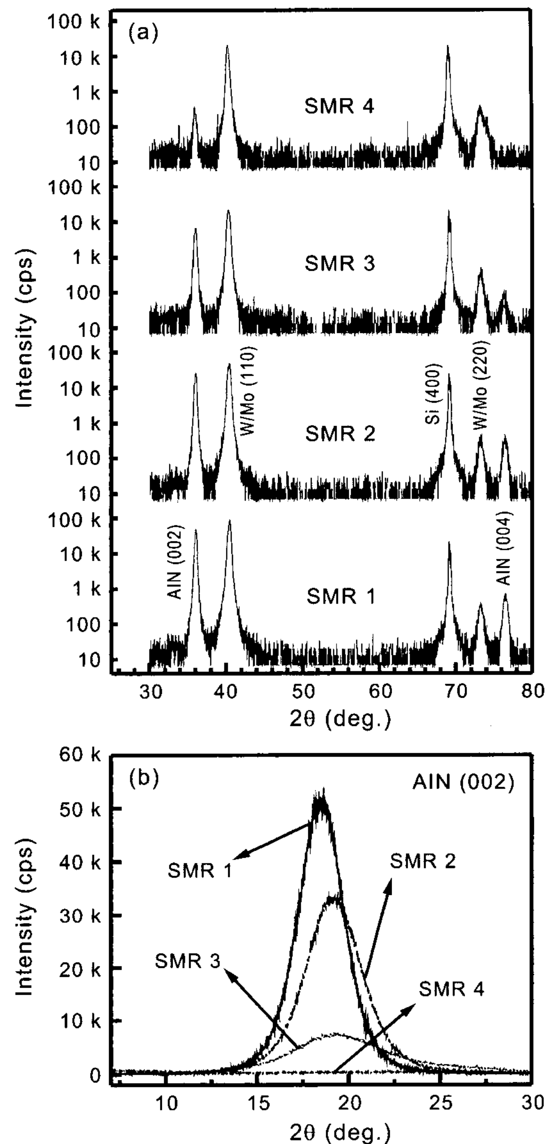

Fig. 1. XRD (a) and AlN (002) plane rocking curve (b) of the various SMRs as a function of Mo electrode deposition pressure as described in Table 1. The degree of AlN c-axis texturing was controlled by the surface conditions of bottom Mo films.

Table 1. Structural and Material Properties of AlN Films, which have Different c-axis Texturing and Mo Based SMRs with 5-layers Reflector Composed of SiO_2 and W in this Study

Specimen	Mo electrodes		(002)-oriented AlN piezoelectric films			5 layers Bragg reflector ($SiO_2/W/SiO_2/W/SiO_2/Si$)	
	thickness	$P_{deposition}$ (mTorr)	thickness	FWHM in ω-scan	estimated acoustic velocity (m/s)	SiO_2 (low Z)	W (high Z)
SMR1	0.2 μm	1	1.57 μm	2.63°	10200	0.53 μm	0.68 μm
SMR2		2.5		3.20°	9950		
SMR3		5		6.05°	9730		
SMR4		10		10.62°	9120		

base, where basic parameters (such as series and parallel resonant frequencies, quality factor (Q) and effective electromechanical coupling coefficient (k_{eff}^2) were extracted from each device data file.

3. Results and Discussion

In order to find only the influence of AlN film quality on the resonance properties of SMRs, piezoelectric AlN and Mo electrode thickness are kept to be same as 1.57 and 0.2 μm in 4 types SMRs, respectively. The Bragg reflector consists of three SiO_2 layers and two W layers. The 0.68-μm-thick W film was chosen as the high acoustic impedance material and the 0.53-μm-thick SiO_2 as the low acoustic impedance material in the Bragg reflector. The c-axis orientation of AlN films, which deposited at the same conditions, was controlled by the different surface conditions of Mo electrodes, as described above. The structural and material properties of four types SMRs were summarized in Table 1.

Fig. 1 show the XRD patterns and AlN (002) plane rocking curve of the SMRs composed of Mo/AlN/Mo and 5-layers Bragg reflector (0.53 μm-SiO_2/0.68 μm-W/SiO_2/W/SiO_2/Si). In the XRD θ-2θ measurement mode, diffraction peaks originating from other AlN planes than (000l) could not be detected in all SMRs. As expected, the intensity of AlN (002) plane increased as decreasing the sputtering pressure in Mo electrode deposition from SMR4 to SMR1. In SMR4, (004) peak was not observed. This difference was attributed to the weak normal alignment to the substrate of the (001) AlN unit cell. The degree of c-axis texturing can be measured by rocking curve. The full widths at half maximum (FWHMs) in rocking curve were 10.62°, 6.05, 3.20, and 2.63° in SMR4, SMR3, SMR2, and SMR1, respectively. Using these differences, it can be investigated that the direct relationship between the crystallographic properties of AlN film between the resonant properties of SMR.

To check and confirm the structural properties, we measured cross-sectional morphologies of SMRs as a function of the Mo sputtering pressure, as shown in Fig. 2(a), (b), (c), and (d) which represented SMR1, SMR2, SMR3, and SMR4, respectively. In all cases, the same Bragg reflector layers were used. It is found that the each layer in SMRs has the nearly same thickness, but only the microstructures of AlN piezoelectric are quite different. As decreasing the degree of c-axis texturing of AlN films, the columnar boundary of AlN films became visible and irregular, as shown in Fig. 2(d).

The S_{11} scattering parameter was measured around the fundamental thickness resonance mode of the SMRs fabricated by using highly textured AlN films deposited on the controlled Mo electrode. The most important figures of merit for a FBAR are the effective coupling coefficient, k_{eff}^2 and the quality factor, Q.[11] The effective coupling coefficient is defined as:

$$k_{eff}^2 = \frac{\dfrac{\pi f_s}{2 f_p}}{\tan\left(\dfrac{\pi f_s}{2 f_p}\right)} \approx \frac{\pi^2}{4} \frac{f_p - f_s}{f_p} \tag{1}$$

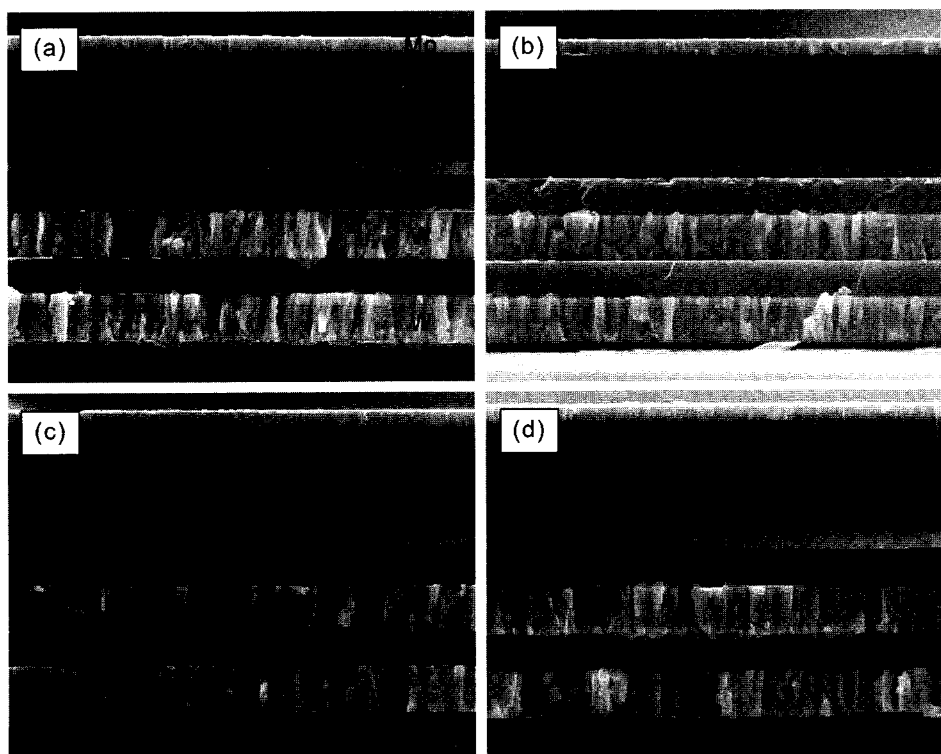

Fig. 2. Cross-sectional SEM of the various SMRs as described in Table 1. The Bragg reflectors are the same but only the crystalline property of AlN films is different. (a) SMR1, (b) SMR2, (c) SMR3, and (d) SMR4.

where the f_p and f_s are the measured parallel and series resonance frequencies which correspond the maximum and minimum impedance point, respectively. k^2_{eff} of a resonator is closely related with the piezoelectric coupling constant (k_t) of AlN piezoelectric films, as below equation at the longitudinal acoustic wave fundamental resonance.

$$k^2_{eff} = \frac{k_t^2}{1+k_t^2} \qquad (2)$$

And, k_t is dependent on the c-axis texturing property of AlN films, which is determined by rocking curve.[2] The Q values of SMR can be calculated by differentiating the impedance phase φ_z:

$$Q_{s,p} = \frac{f_{s,p}}{2}\frac{\partial \varphi_Z}{\partial f}\bigg|_{f=f_{s,p}} \qquad (3)$$

which is to be evaluated at the series and parallel resonance frequencies. The corresponding impedance magnitude (Z) and impedance phase of SMR1 and SMR4 are displayed in Fig. 3(a) and (b), respectively. These two SMRs had the big difference of AlN c-axis texturing property, as described Table 1. As a consequence, the gap between f_p and f_s in SMR1 and SMR4 was about 46 and 20 MHz, respectively. In spite of the same thickness, the resonance frequencies were also different, which correspond to the different acoustic velocity of (002)-oriented AlN films. From the mathematical analysis based on a fundamental one-dimensional Bulk Acoustic Wave(BAW) composite resonator expression,[12] we estimated the acoustic velocity of AlN films with different orientation. The acoustic velocity, as shown in Table 1, was decreased as decreasing the degree of c-axis texturing. The longitudinal acoustic velocity of c-axis textured AlN film was estimated to be about 9120 to 10200 m/s.

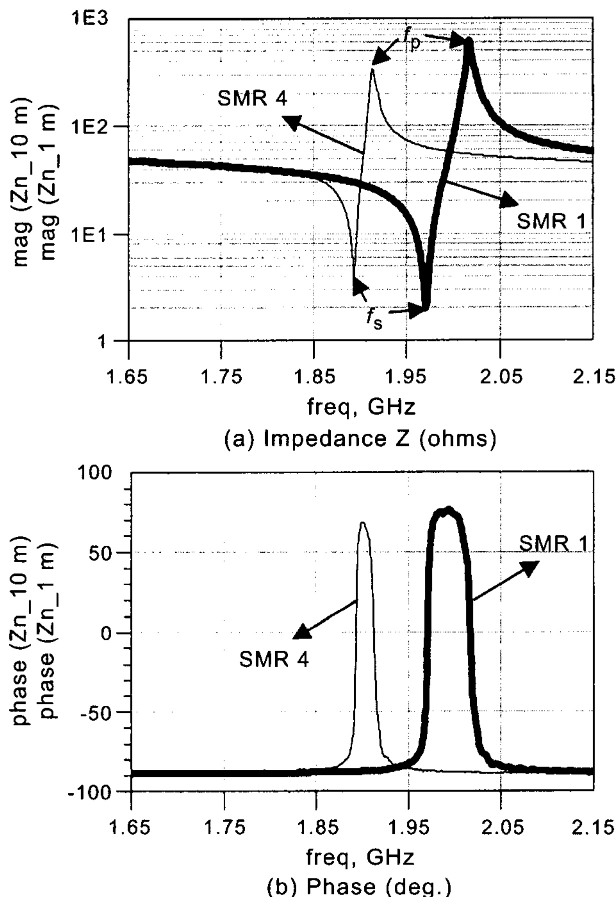

Fig. 3. Narrow band impedance magnitude (a) and phase (b) of the two SMRs having different degree of c-axis texturing property. The values of FWHM in AlN (002) rocking curve of SMR1 and SMR4 were 2.63° and 10.62°, respectively.

Fig. 4(a) showed the relationship between (k^2_{eff}) and the degree of c-axis texturing of AlN films. As decreasing the FWHM of (002) plane by rocking curve and enhancing the c-axis texturing, k^2_{eff} and k_t increased gradually. In SMR1 with a rocking curve FWHM of 2.63°, k^2_{eff} of 5.5% was calculated from the fundamental resonance. In this case, the piezoelectric coupling constant (k_t) of AlN piezoelectric films was 0.24, which comparable to the intrinsic value of 0.25.[13]

For band pass filter for PCS and WLAN, the minimum bandwidth is requested such as 60 and 200 MHz, respectively.[14,15] To meet this specification, k^2_{eff} of SMRs should be above 5%. One can find from Fig. 4(a) that this requirement is satisfactory if the value of FWHM is below 4 degree. On

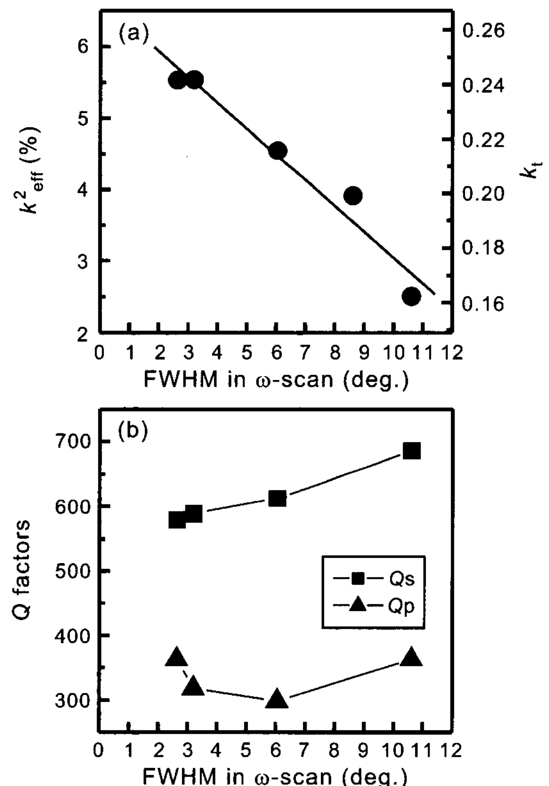

Fig. 4. Effective electromechanical coupling coefficient (k^2_{eff}) and piezoelectric coupling constant (k_t) (a) and Q factors (b) of the various SMRs as a function of AlN (002) rocking curve FWHM.

the other hand, the quality factor Q_s and Q_p at series resonance and parallel resonance do not seem to be dependent on the AlN film texturing property, as shown in Fig. 4(b). These results might be considered as the more complex origins of quality factor, such as the quarter-wavelength mismatch of Bragg reflector resulting from film uniformity problem, the different resonance frequency, electrical loss and acoustic wave propagation loss.[16]

4. Conclusions

The relationship between k^2_{eff} of SMRs and the degree of AlN c-axis orientation was investigated in this study. As increasing the degree of c-axis texturing in AlN films, the k^2_{eff} in resonators increased gradually. In the case of the AlN piezoelectric thin film with a rocking curve FWHM of 2.63°, k^2_{eff} and piezoelectric coupling constant (k_t) were to be 5.5% and 0.24, respectively. It was found that the least FWHM of 4°, which corresponds to k^2_{eff} of above 5%, was necessary in application for personal communication system and wireless local area network band pass filters. The longitudinal acoustic wave velocity of AlN films was also decreased as decreasing the degree of c-axis texturing. In c-axis textured AlN film showing a FWHM of 2.63°, the acoustic wave velocity was about 10200 m/s.

Acknowledgment

This work was supported by the Korea Ministry of Commerce, Industry and Energy under the Advanced Transceiver System Development Program.

REFERENCES

1. K. M. Lakin, G. R. Kline, and K. T. McCarron, "Development of Miniature Filters for Wireless Application," *IEEE Trans. Microwave Theory Tech.*, **43** [12] 2933-39 (1995).
2. K. M. Lakin, "Thin-film Resonators and Filters," *IEEE Proceedings on Ultrasonics Symposium*, 895-906 (1999).
3. M.-A. Dubois, P. Muralt, and V. Plessky, "BAW Resonators Based on Aluminum Nitride Thin Films," *IEEE Proceedings on Ultrasonics Symposium*, 907-10 (1999).
4. K. M. Lakin, J. R. Belsick, J. P. McDonald, K. T. McCarron, and C. W. Andrus, "Bulk Acoustic Wave Resonators and Filters for Applications Above 2 GHz," *IEEE MTT-S Int. Microwave Symp. Dig.*, 1487-90 (2002).
5. J. Kaitila, M. Ylilammi, J. Molarius, J. Ella, and T. Makkonen, "ZnO Based Thin Film Bulk Acoustic Wave Filters for EGSM Band," *IEEE Proceedings on Ultrasonics Symposium*, 803-06 (2001).
6. P. B. Kirby, Q. X. Su, E. Komuro, Q. Zhang, M. Imura, and R. Whatmore, "PZT Thin Film Bulk Acoustic Resonators and Filters," *IEEE Proceedings on International Frequency Control Symposium and PDA Exhibition*, 687-94 (2001).
7. M.-A. Dubois and P. Muralt, "Measurement of the Effective Transverse Piezoelectric Coefficient $e_{31,f}$ of AlN and Pb$(Zr_x,Ti_{1-x})O_3$ Thin Films," *Sensors and Actuators*, **77** 106-12 (1999).
8. R. S. Naik, J. J. Lutsky, R. Reif, C. G. Sodini, A. Becker, L. Fetter, H. Huggins, R. Miller, J. Pastalan, G. Rittenhouse, and Y.-H. Wong, "Measurements of the Bulk. C-axis Electromechanical Coupling Constant as a Function of AlN Film Quality," *IEEE Trans. Ultrason. Ferroelectr. Freq. Control*, **47** [1] 292-96 (2000).
9. S.-H. Lee, J.-K. Lee, and K. H. Yoon, "Growth of Highly c-axis Textured AlN Films on Mo Electrodes for Film Bulk Acoustic Wave Resonators," *J. Vac. Sci. Technol.* A. **21** [1] 1-5 (2003).
10. S.-H. Lee, J.-K. Lee, S.-H. Kim, J.-H. Kim, and K. H. Yoon, "AlN-Si Thin Film Bulk Acoustic Over-moded Resonator," *J. Kor. Ceram. Soc.*, **37** [12] 1198-203 (2000).
11. K. M. Lakin, G. R. Kline, and K. T. McCarron, "High-Q Microwave Acoustic Resonators and Filters," *IEEE Trans. Microwave Theory and Tech.*, **41** [12] 2139 (1993).
12. G. S. Kino, Acoustic Waves: Devices, Imaging, and Analog signal processing; p. 32, Prentice-Hall Inc., Englewood Cliffs, NJ, 1987.
13. O. Ambacher, "Growth and Applications of Group III-nitrides," *J. Phys.* D, **31** 2653 (1998).
14. K. M. Lakin, K. T. MaCarron, J. Belsick, and R. Rose, "Filter Banks Implemented with Integrated Thin Film Resonators," *IEEE Proceedings on Ultrasonics Symposium*, 851-54 (2000).
15. T. Nishihara, T. Yokoyama, T. Miyashita, and Y. Satoh, "High Performance and Miniature Thin Film Bulk Acoustic Wave Filters for 5 GHz," IEEE Proceedings on Ultrasonics Symposium, Presented (2002).
16. S.-H. Lee, K. H. Yoon, and J.-K. Lee, "Influence of Electrode Configurations on the Quality Factor and Piezoelectric Coupling Constant of Solidly Mounted Bulk Acoustic Wave Resonators," *J. Appl. Phys.*, **92** [7] 4062-69 (2002).